UNITED STATES
NAVAL POSTGRADUATE SCHOOL

APPLICATION OF THE KALMAN FILTER TO SPHERICAL DISCRETE TRACK SMOOTHING AND PREDICTION

by

J. S. Demetry

R. E. Hudson

1 September 1966

TECHNICAL REPORT/RESEARCH PAPER NO. 70

UNITED STATES NAVAL POSTGRADUATE SCHOOL
Monterey, California

Rear Admiral E. J. O'Donnell, USN
Superintendent

R. F. Rinehart
Academic Dean

ABSTRACT:

This paper investigates the effectiveness of a method for circumventing the problem of nonlinear observation of a linear system's state variables in the Kalman filter discrete estimation scheme. The method employs a linearization of the nonlinear coordinate transformation, in this case cartesian to spherical. The performance of a filter designed by this method is observed as a function of measurement error, accuracy of filter initialization, and the relevance of the estimated initial error covariance, $P_{2|1}$. The investigation reveals that the most critical factor in filter performance and stability is filter state initialization.

This task was supported by: Naval Air Development Center

Prepared by: J. S. Demetry
Assistant Professor of Electrical Engineering

R. E. Hudson
Lieutenant United States Navy

Approved by:

C. H. Rothauge

Chairman, Department of

Electrical Engineering

Released by:

C. E. Menneken

Dean of

Research Administration

U. S. Naval Postgraduate School Technical Report/Research Paper No. 70

UNCLASSIFIED

TABLE OF CONTENTS

1.0	Introduction	1
2.0	Linearization of the Coordinate Transformation	2
3.0	Filter Simulation	4
3.1	Target Track and Dynamics	4
3.2	Example 1	6
3.3	Example 2	11
3.4	Example 3	13
3.5	Example 4	15
4.0	Conclusion	18

APPLICATION OF THE KALMAN FILTER TO SPHERICAL DISCRETE TRACK SMOOTHING AND PREDICTION

1.0 Introduction

The Kalman filter is capable of estimating the state variables of a linear dynamic system under conditions of random perturbation of that system and noisy observation of a linear combination or combinations of the state variables. The motion of an airborne target, though presumably describable by linear dynamic equations in a cartesian frame, is most often observed in a spherical coordinate frame, as is the case in radar tracking. The transformation from cartesian to spherical coordinates is of course a nonlinear transformation, and does not allow the formulation of a constant observability matrix as required to the implementation of the Kalman estimation scheme.

This paper investigates the effectiveness of a method for circumventing the problem of nonlinear observation of a linear system's state variables. The method employs a linearization of the cartesian-to-spherical coordinate transformation. The performance of a filter designed by this method is observed as a function of measurement error, accuracy of filter initialization, and the relevance of the estimated initial error covariance, $P_{2|1}$.

The investigation reveals that the most critical factor in filter performance and stability is filter state initialization. The filter performs remarkably well, even in the face of considerable measurement error, provided it gets a "good start", i.e., a fairly accurate initialization of the filter states. The linearization scheme yields instability, however, for poor initialization. This is rather

unfortunate since in a realistic situation the accuracy of initialization is a direct function of measurement error. The results underscore the need for more powerful initialization schemes for use in this and related nonlinear filtering problems.

Included are digital computer simulations of filter performance.

2.0 Linearization of the Coordinate Transformation

Figure 1 represents in block diagram form the discrete state transition equations for the dynamic process and the Kalman filter. All operations within the dotted contour are carried out in cartesian coordinates. The observability transformation operator T is the nonlinear cartesian-to-spherical coordinate transformation. The filter gain matrix G assumes and in fact requires for its calculation a linear observability matrix H. Such a matrix is obviously absent in the present problem.

The linearization proceeds from the observation that the quantity

$$\underset{\sim}{x}_k \triangleq \underset{}{x}_k - \hat{\underset{}{x}}_{k \mid k-1} \tag{1}$$

is the difference between two hopefully similar quantities, and may thus be classified as a "small difference". Dropping the subscripts from equation (1) for convenience and re-arranging,

$$\hat{\underset{}{x}} = \underset{}{x} - \underset{\sim}{x} \tag{2}$$

We now note that

$$\hat{\underset{}{z}} = T\left[\hat{\underset{}{x}}\right] = T\left[\underset{}{x} - \underset{\sim}{x}\right] \tag{3}$$

A Taylor series expansion of equation (3) about $\underset{}{x}$ yields

$$\hat{\underset{}{z}} = T\left[\underset{}{x}\right] - \frac{\partial T}{\partial \underset{}{x}}\Big|_{\underset{}{x}} \underset{\sim}{x} + \text{----} \tag{4}$$

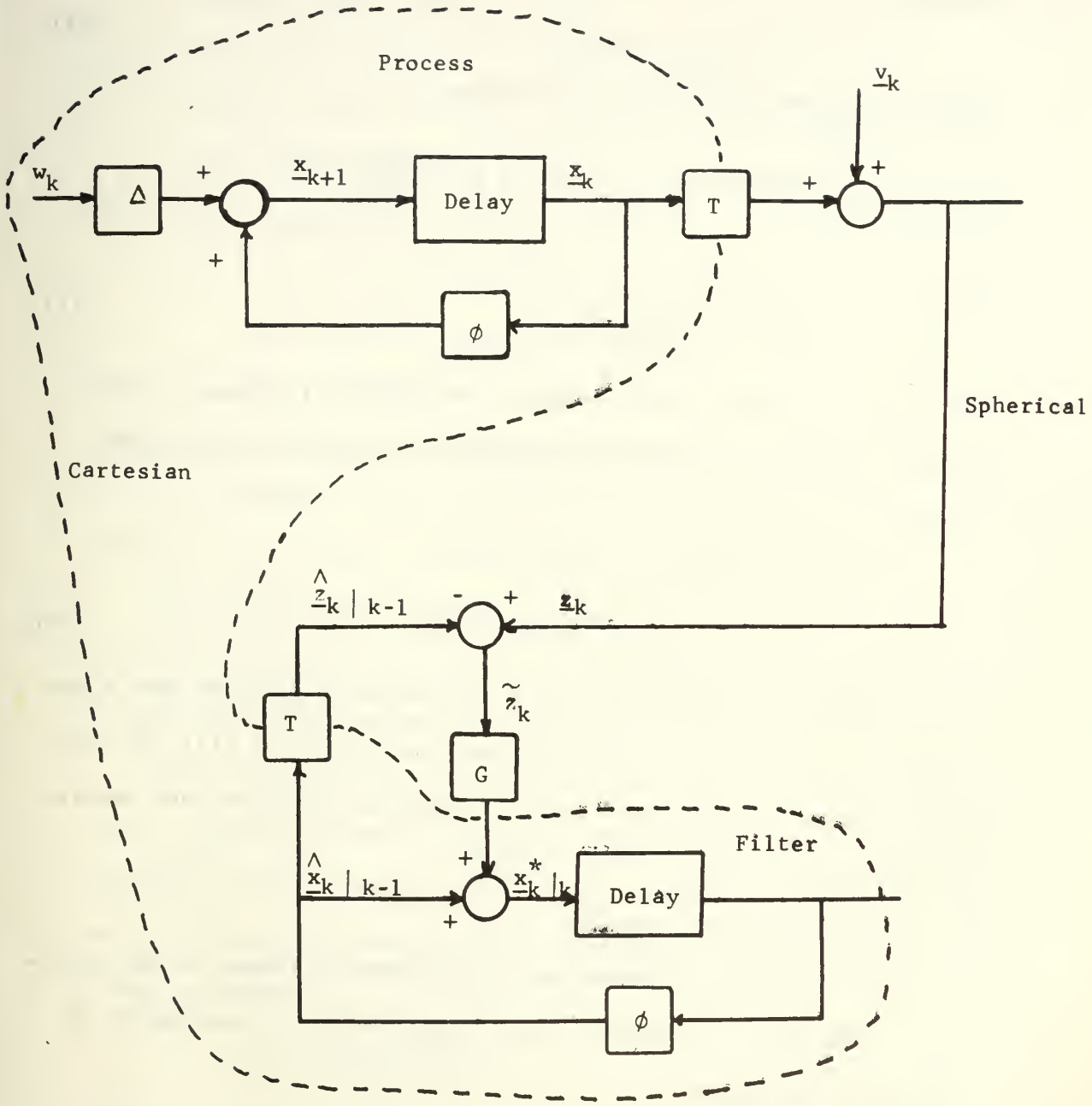

Figure 1. Block diagram of the dynamic process and the Kalman filter estimating the state variables of that process.

where the higher-order derivatives have been dropped. We may also write

$$\tilde{\underline{z}} = \underline{z} - \hat{\underline{z}} \tag{5}$$

Noting that

$$\underline{z} = T[\underline{x}] + \underline{v} \tag{6}$$

equation (5) combined with (4) will give

$$\tilde{\underline{z}} = T[\underline{x}] + \underline{v} - \left\{ T[\underline{x}] - \frac{\partial T}{\partial \underline{x}} \Big|_{\underline{x}} \tilde{\underline{x}} \right\}$$

or

$$\tilde{\underline{z}} = \underline{v} + \frac{\partial T}{\partial \underline{x}} \Big|_{\underline{x}} \tilde{\underline{x}} \tag{7}$$

The role of the partial derivative in equation (7) is seen by comparison with the corresponding equation for linear observability, namely

$$\tilde{\underline{z}} = H\underline{x} + \underline{v} - H\hat{\underline{x}}$$

or

$$\tilde{\underline{z}} = \underline{v} + H(\underline{x} - \hat{\underline{x}}) = \underline{v} + H\tilde{\underline{x}} \tag{8}$$

The partial of T with respect to $\underline{x}$, evaluated at $\hat{\underline{x}}$ rather than $\underline{x}$ because the latter is not available, may now be used to fill the role of H in the calculation of the filter gain matrix G for each sample.

3.0 Filter Simulation

3.1 Target Track and Dynamics

The true target information that follows is common to all subsequent examples. It assumes the tracking radar to be carried by an airborne interceptor.

Initial target position	North 60 miles
	East 10 miles
	Down 2 miles
Initial target heading	180^{o}
Interceptor heading	000^{o} throughout
Initial target velocity	0.1473 miles per second
Interceptor velocity	0.148 miles per second, throughout

The target executes the following maneuver:

at t = 106 seconds, acceleration as follows

North +0.001715 miles per second^2

East -0.00474 miles per second^2

This acceleration continues for twenty seconds, at which time the target is headed 220^{o} with a velocity of 0.1473 miles per second. The duration of the run is 180 seconds.

Observations are taken every two seconds. The target dynamics in each of the three cartesian coordinates have been represented by $\frac{1}{s^3}$, with all three motions assumed uncoupled.

No attempt was made either to estimate or to sense target maneuvers. The filter was kept "open" to the possibility of maneuvers by assigning, for purposes of filter gain calculation, an arbitrarily small variance to the random disturbance w_k. The resulting non-zero Q matrix, where

$$Q = \Delta \, E \left[w_k^2 \right] \Delta^T \tag{9}$$

effectively prohibits the convergence of filter gains to zero, and hence keeps active the link between the target and the filter.

At each observation, it was necessary to solve, in addition to the conversion, dynamic, smoothing and prediction equations implied by Figure 1, each of the following equations for determination of the filter gains:

$$G_k = P_{k \mid k-1} M_k^t \left[M_k P_{k \mid k-1} M_k^t + R \right]^{-1} \tag{10}$$

$$P_{k+1 \mid k} = \phi \left[P_{k \mid k-1} - G_k M_k P_{k \mid k-1} \right] \phi^T + Q \tag{11}$$

$P_{k \mid k-1}$ is the covariance matrix of prediction error. The M_k matrix is found as

$$M_k = \frac{\partial T}{\partial x} \Big|_{\underline{x} = \hat{\underline{x}}_{k \mid k-1}} \tag{12}$$

and must be evaluated at every observation. R is simply the covariance matrix of spherical observation noise.

3.2 Example 1

In example 1, the radar observables are range, range rate, and the two angles θ and ϕ, as depicted in Figure 2. The standard deviations for spherical observation noise are as follows:

σ_{range} = 1.437 miles

σ_{θ} = 0.0035 radians

σ_{ϕ} = 0.0174 radians

$\sigma_{\dot{r}}$ = 0.00152 miles/second

Linearization of the coordinate transformation

$$r = \sqrt{N^2 + E^2 + D^2} \tag{13}$$

$$\theta = \tan^{-1} \frac{E}{N} \tag{14}$$

$$\phi = \frac{D}{\sqrt{N^2 + E^2}} \tag{15}$$

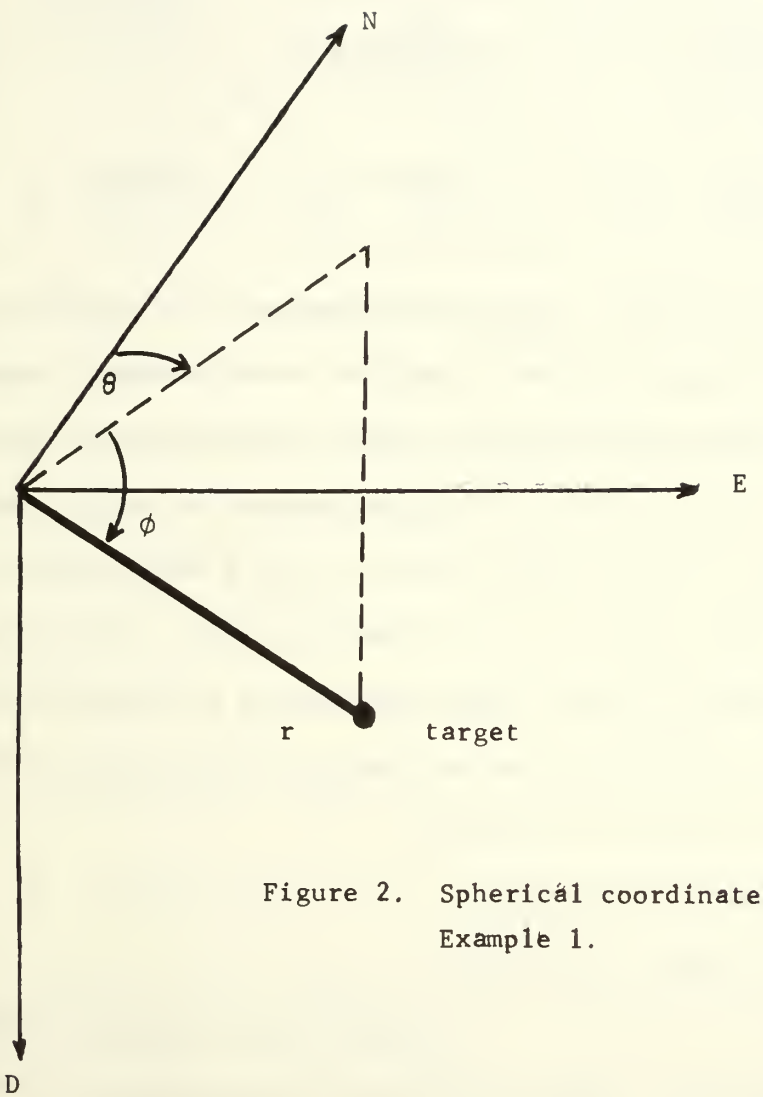

Figure 2. Spherical coordinates for Example 1.

$$\dot{r} = \frac{N\dot{N} + E\dot{E} + D\dot{D}}{r} \tag{16}$$

yielded

$$M = \begin{bmatrix} \frac{N}{r} & 0 & 0 & \frac{E}{r} & 0 & 0 & \frac{D}{r} & 0 & 0 \\ \frac{-E}{N^2 + E^2} & 0 & 0 & \frac{N}{N^2 + E^2} & 0 & 0 & 0 & 0 & 0 \\ \frac{-ND}{r^2\sqrt{N^2 + E^2}} & 0 & 0 & \frac{-DE}{r^2\sqrt{N^2 + E^2}} & 0 & 0 & \sqrt{N^2 + E^2} & 0 & 0 \\ \frac{r^2\dot{N} - N\alpha}{r^3} & \frac{N}{r} & 0 & \frac{r^2\dot{E} - E\alpha}{r^3} & \frac{E}{r} & 0 & \frac{r^2\dot{D} - D\alpha}{r^3} & \frac{D}{r} & 0 \end{bmatrix} \tag{17}$$

where $\alpha = N\dot{N} + E\dot{E} + D\dot{D}$. The filter cartesian state variables were initialized by inversion of the coordinate transformation through velocity, using first differences from the initial two observations where necessary. Although, as will be shown, the initialization and bootstrapping employed in this example failed in some cases to yield a stable track, it is now described in some detail as an illustration of the difficulties encountered in initialization. The observations are numbered starting with 1. The following expressions describe the starting procedure. The variables are as shown in Figure 1.

a) Observation 1 yields $\underline{z}_1$

b) Observation 2 yields $\underline{z}_2$

c) Inverse coordinate transformation and first differences on observations 1 and 2 yield position and velocity in all three cartesian coordinates. Accelerations are arbitrarily set to

zero. The filter cartesian states $\underline{x}^*_{2 \mid 2}$ are now set to these values.

d) $\hat{\underline{x}}_{3 \mid 2}$ is calculated

e) $\hat{\underline{z}}_{3 \mid 2}$ is calculated

f) $M_2 = \frac{\partial T}{\partial x} \Big|_{\underline{x} = \underline{x}^*_{2 \mid 2}}$ is calculated

g) G_2 and $P_{3 \mid 2}$ are calculated as in equations (10) and (11), using $P_{2 \mid 1}$, the initializing value of prediction error covariance, and M_2. It would appear that a further smoothing of filter states would now be possible, since a filter gain matrix G_2 has been calculated. We note, however, that there has not been generated an $\underline{x}^*_{1 \mid 1}$ upon which $\hat{\underline{x}}_{2 \mid 1}$ and $\hat{\underline{z}}_{2 \mid 1}$ depend. Without the latter we cannot generate $\tilde{\underline{z}}_2 = \underline{z}_2 - \hat{\underline{z}}_{2 \mid 1}$. It is for this reason that the first smoothing is deferred to the third observation.

h) $M_3 = \frac{\partial T}{\partial x} \Big|_{\underline{x} = \hat{\underline{x}}_{3 \mid 2}}$

i) G_3 and $P_{4 \mid 3}$ are calculated from $P_{3 \mid 2}$ and M_3

j) Observation 3 yields $\underline{z}_3$

k) Smoothing occurs, $\underline{x}^*_{3 \mid 3} = \hat{\underline{x}}_{3 \mid 2} + G_3 (\underline{z}_3 - \hat{\underline{z}}_{3 \mid 2})$

Bootstrapping is now complete, and the filter operates from this point on in a straight forward fashion.

It is not implied and not to be inferred that this initialization and

bootstrapping scheme is more effective or more desirable than any one of many other such methods. Serious questions can, in fact, be raised about the fact that the initializing value $P_{2|1}$ is not the one used in the first smoothing. The first filter gain used, G_3, is based upon $P_{3|2}$, a calculated value. It is for these reasons that subsequent examples will attempt, insofar as possible, to isolate the effects of observation noise, error covariance initialization, and filter state initialization.

Returning now to example 1, there remains only to note that $P_{2|1}$ was chosen as

$$P_{2|1} = \begin{bmatrix} 5 & & & & & & \\ & 1 & & & & & \\ & & 1 & & & & \\ & & & 5 & & & \\ & & & & 1 & & \\ & & & & & 1 & \\ & & & & & & 5 \\ & & & & & & & 1 \\ & & & & & & & & 1 \end{bmatrix} \tag{18}$$

The raw radar data and the smoothed track for the NE plane, both compared with the true track (as seen from the interceptor) are shown in Figure 3. This run was chosen as example 1 because it typifies the transition from stable to unstable filter performance for the initialization scheme outlined above. The smoothed track shows evidence of indecision in the early stages, an indecision that becomes instability for higher observation noise levels. The filter is observed to be quite effective for the better part of the track. Runs performed at lower noise yielded virtually immediate lock-on to a very satisfactory smoothed track.

3.3 Example 2

Example 2 seeks to isolate the effect of measurement noise upon filter performance. The first step taken here was to bypass the bootstrapping procedure. This was accomplished by starting the program at step h) in the bootstrap outline given above. $\hat{\underline{x}}_{3 \mid 2}$ was set equal to the true $\underline{x}_3$, while $P_{3 \mid 2}$, the covariance of prediction error associated with $\hat{\underline{x}}_{3 \mid 2}$, was properly set to zero. Hence the filter is getting not only an error-free start with respect to the first set of predicted filter states, but a precise corresponding conditional covariance initialization as well. This effectively isolates measurement noise as a variable in the problem. The initial value of zero for covariance acts to effectively shut off filter gains until the P matrix starts accumulating value from the nominally small value of Q. This process of growth for the P and G matrices is readily seen by inspection of equations (10) and (11). The low initial values of G allow the error-free initial filter states to proceed very nearly along the true track, virtually free of any correction arising from observation noise, until such time as P has grown to an appreciable level.

Nine runs are presented in this example. In the first run, the measurement noise standard deviations are one-tenth of the corresponding values in example 1. In each of the eight subsequent runs, the standard deviations are increased by a factor of 2. Figure 4 shows the set of 9 smoothed tracks, shown with the true track, for the NE plane. The corresponding raw observed tracks are not included, but an appreciation for these tracks might be obtained by noting that the raw track

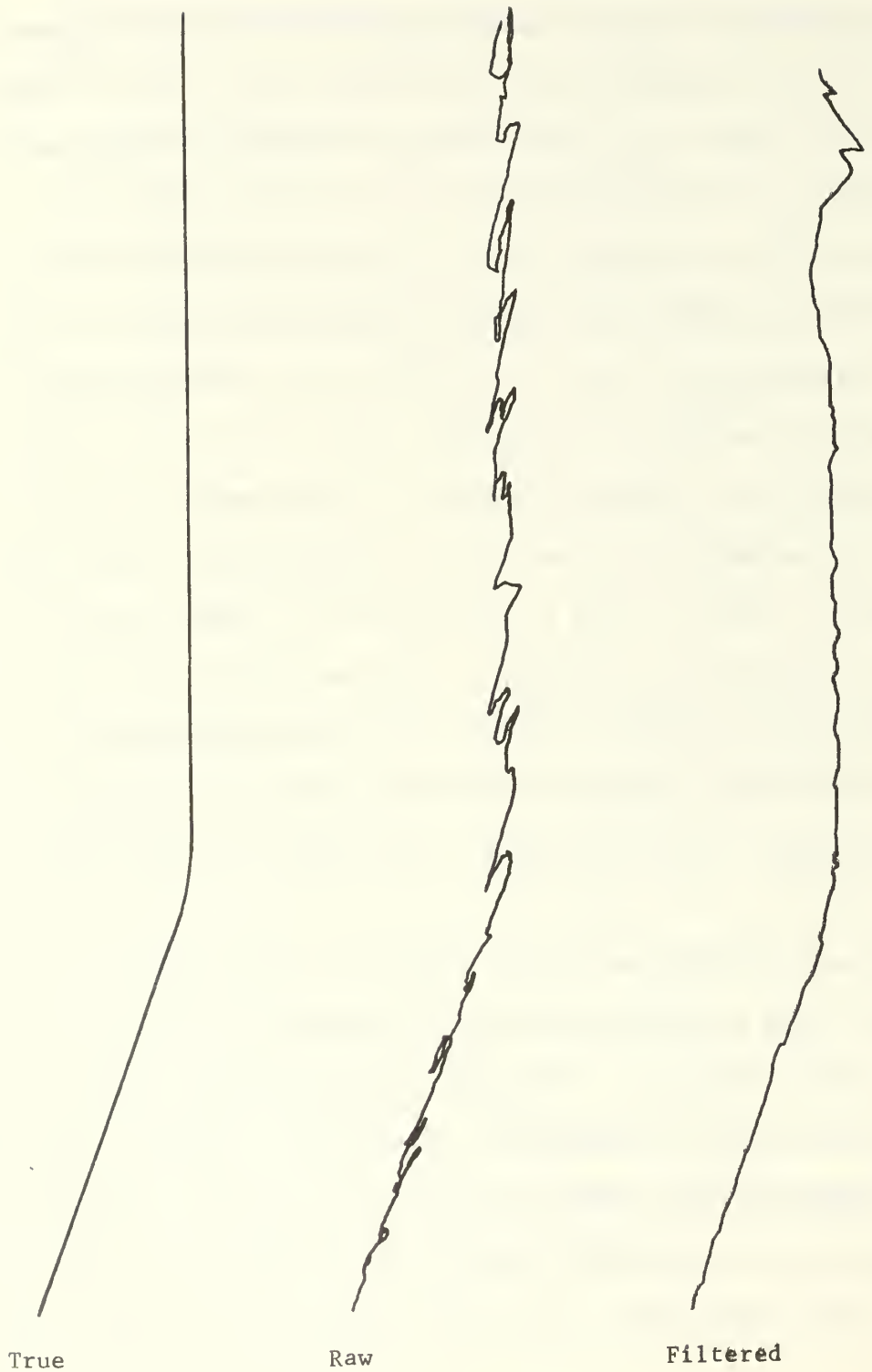

Figure 3. True, raw, and filtered tracks, NE plane, for Example 1. Scale: 7 miles per inch.

of Figure 3, example 1, would fit roughly between the raw tracks underlying smoothed tracks 4 and 5 of Figure 4. We may further note that the raw track for run 9, Figure 4, is roughly 25 times as noisy as that shown in Figure 3a.

We can only conclude from the results of example 2 that an ever-increasing level of measurement noise is not of itself sufficient to render the filter unstable, at least in the case of error-free state and covariance initialization. This tends to indict filter state initialization and/or conditional covariance initialization as the weak points leading to instability. This is looked into in example 3.

3. Example 3

In example 3, observation noise levels are identical for each of seven runs and are equal to those given in example 1. The starting bootstrap was once again bypassed. In the first run the filter was given an error-free start, ($\hat{\underline{x}}_{3 \mid 2} = \underline{x}_3$), and $P_{3 \mid 2}$ was accordingly set equal to zero. In the subsequent six runs, increasingly larger state initialization errors were introduced, while concurrently $P_{3 \mid 2}$ was incremented to accurately reflect this increase. In run 2, $P_{3 \mid 2}$ was set to four-hundredths of the value shown in equation (18) and was in each subsequent run increased by a factor of four. In runs 2 through 7, the random number generation subroutine, serving as a source of error for both initialization and measurement noise, was re-initialized so as to produce for each run the same base state initialization error vector and the same sequence of measurement errors. Hence all state initializations lie on the same vector, differing only in magnitude.

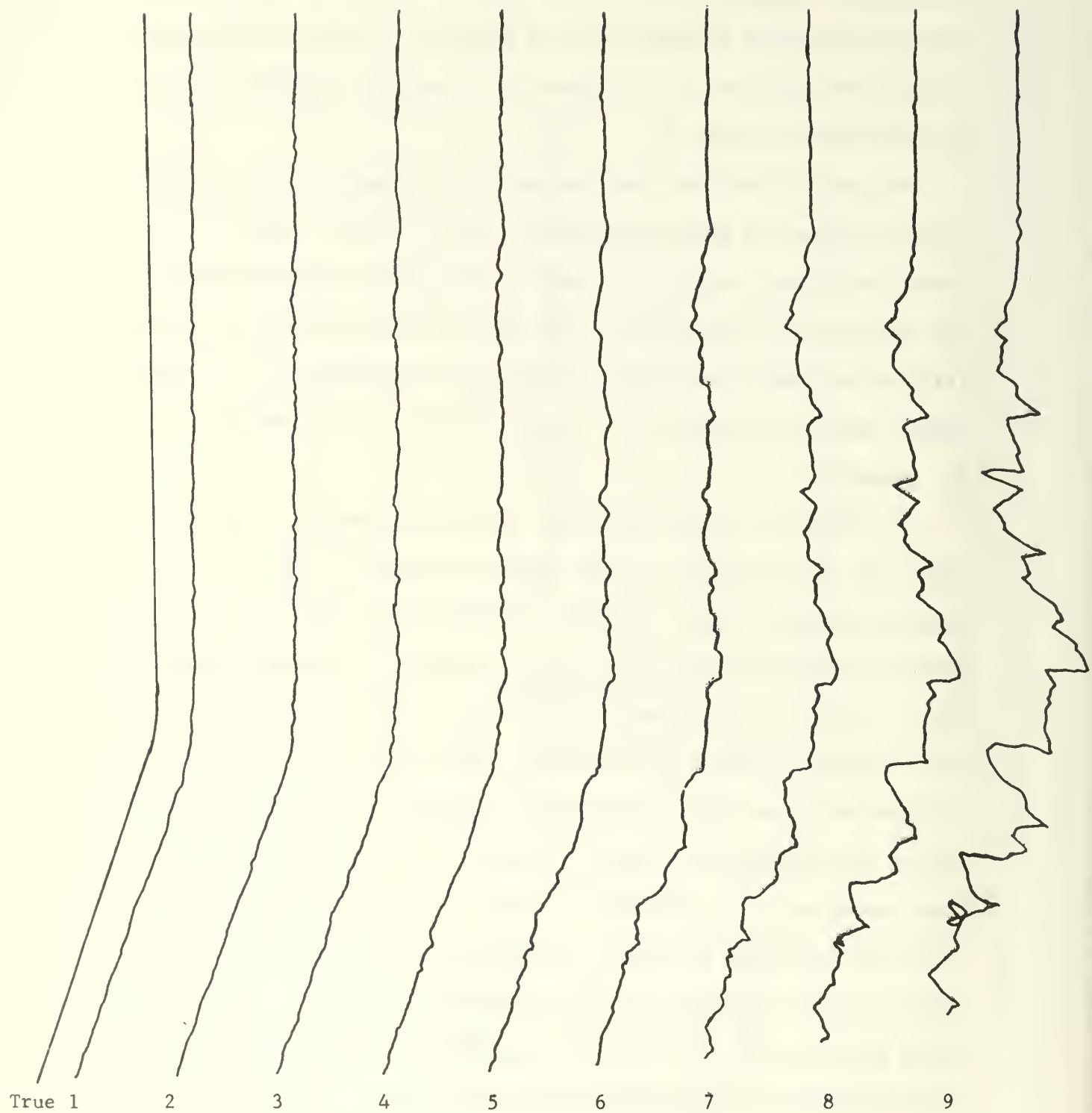

Figure 4. True and filtered tracks, NE plane, for Example 2.
Scale: 7 miles per inch

Figure 5 shows the smoothed track in the NE plane for all seven runs of example 3. The raw track for each run is identical to that of Figure 3. The true track is, of course, also identical to that of Figure 3.

We may conclude from the results of example 3 that accurate covariance initialization does not of itself remove the possibility of filter instability.

State initialization, then, appears to be especially critical.

3.5 Example 4

One final example was chosen to investigate the possibility that the fixed direction of the initial state error vector of example 3 might have been a misleading factor in arriving at the conclusions drawn. Nine runs were made in example 4, with all conditions identical to those of run 4 in example 3 except for the fact that the random number subroutine was not re-initialized for each run. This produced the ensemble of smoothed tracks for the NE plane, shown in Figure 6. These tracks have been grouped to show those considered good, poor, and unstable.

We may conclude from example 4 that although the covariance initialization may accurately reflect the statistical properties of initial state errors, individual samples of the latter may be quite far removed from the mean, adding another degree of sensitivity to the initialization problem. No effort was made to establish a correlation between the tracks of Figure 6 and the extent of dispersion in the nine different initial state error vectors drawn from the same Gaussian distribution.

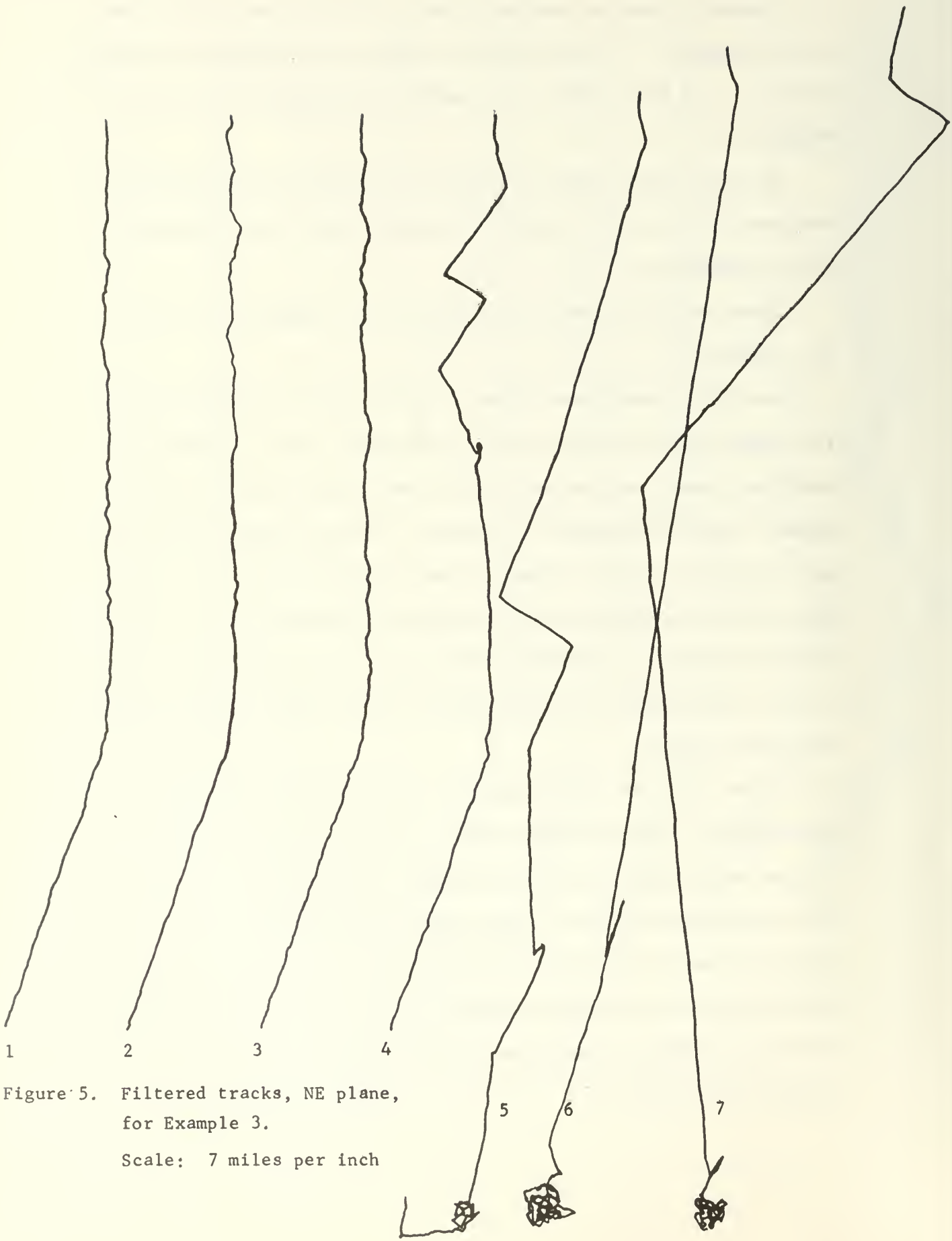

Figure 5. Filtered tracks, NE plane, for Example 3.

Scale: 7 miles per inch

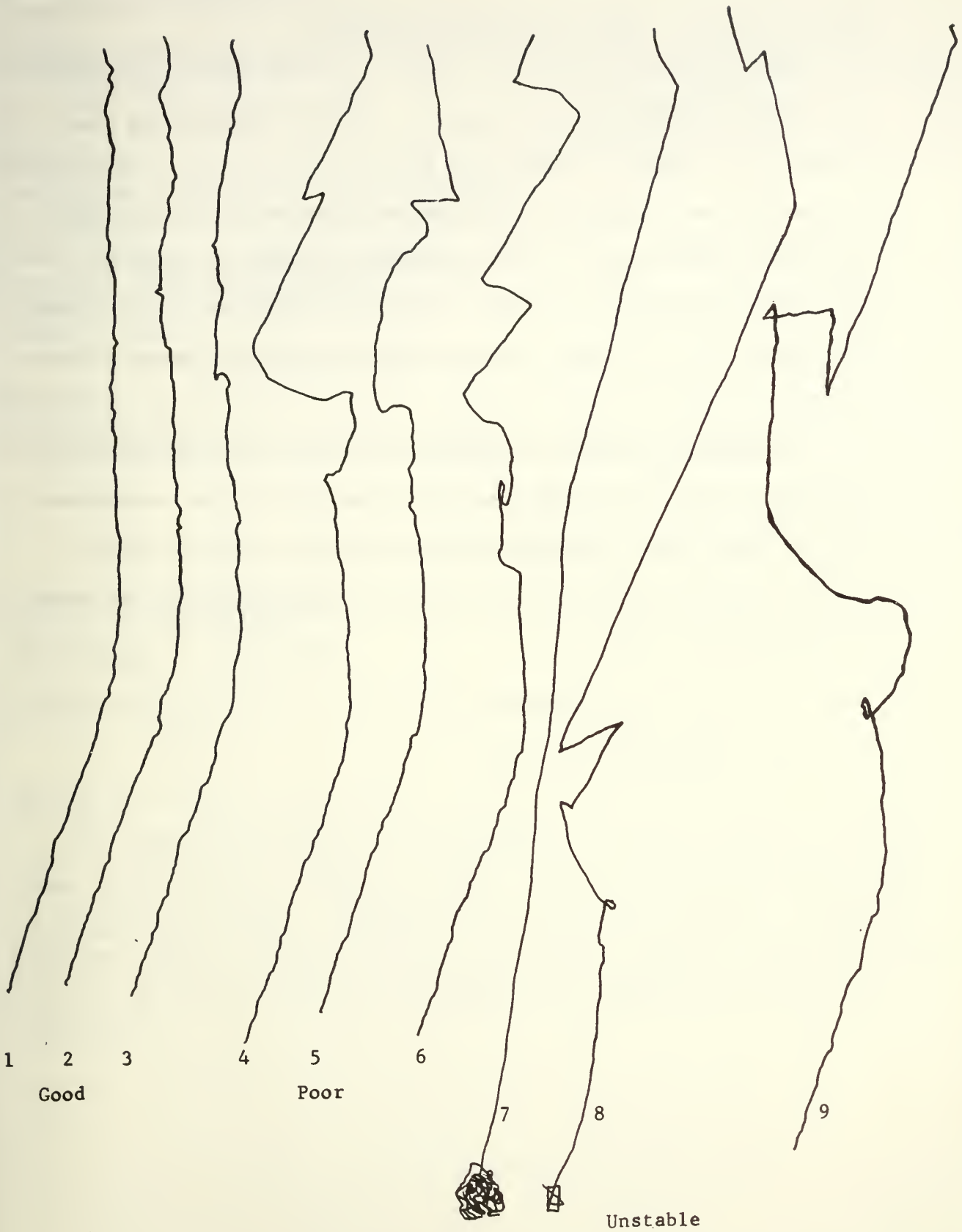

Figure 6. Filtered tracks, NE plane, for Example 4.

Scale: 7 miles per inch.

4.0 Conclusion

Filter state initialization appears to be the most critical factor in filter performance and stability. A bootstrap starting procedure, to be effective, must place the initial state vector within certain bounds. Although no algorithm is presented for analytically determining these bounds, their existence is evident in Figure 5, where filter performance is seen to deteriorate starting with run four. The bounds are very likely strongly dependent upon measurement noise levels.

An effective bootstrap procedure must also include the means of determining meaningfully all elements of the initial error covariance matrix. This is not a simple task, mainly because nonlinear observability leads to dependence between initial state estimates, and hence a full initial P matrix.

Security Classification

DOCUMENT CONTROL DATA - R&D

(Security classification of title, body of abstract and indexing annotation must be entered when the overall report is classified)

1. ORIGINATING ACTIVITY *(Corporate author)*

U. S. Naval Postgraduate School
Monterey, California

2a. REPORT SECURITY CLASSIFICATION

UNCLASSIFIED

2b GROUP

3. REPORT TITLE

Application of the Kalman Filter to Spherical Discrete Track Smoothing and Prediction

4. DESCRIPTIVE NOTES *(Type of report and inclusive dates)*

Technical Report/Research Paper

5. AUTHOR(S) *(Last name, first name, initial)*

Demetry, James S.
Hudson, Ralph E.

6. REPORT DATE	7a. TOTAL NO. OF PAGES	7b. NO. OF REFS
1 September 1966		

8a. CONTRACT OR GRANT NO.	9a. ORIGINATOR'S REPORT NUMBER(S)
b. PROJECT NO.	TR/RP 70
c.	9b. OTHER REPORT NO(S) *(Any other numbers that may be assigned this report)*
d.	

10. AVAILABILITY/LIMITATION NOTICES

Distribution of this document is unlimited

11. SUPPLEMENTARY NOTES	12. SPONSORING MILITARY ACTIVITY
	Naval Air Development Center

13. ABSTRACT

This paper investigates the effectiveness of a method for circumventing the problem of nonlinear observation of a linear system's state variables in the Kalman filter discrete estimation scheme. The method employs a linearization of the nonlinear coordinate transformation, in this case cartesian to spherical. The performance of a filter designed by this method is observed as a function of measurement error, accuracy of filter initialization, and the relevance of the estimated initial error covariance, $P_{2|1}$. The investigation reveals that the most critical factor in filter performance and stability is filter state initialization.

DD FORM 1 JAN 64 1473

D23558

UNCLASSIFIED
Security Classification

14. KEY WORDS	LINK A		LINK B		LINK C	
	ROLE	WT	ROLE	WT	ROLE	WT
Estimation Filter Kalman filter Coordinate transformation linearization						

INSTRUCTIONS

1. ORIGINATING ACTIVITY: Enter the name and address of the contractor, subcontractor, grantee, Department of Defense activity or other organization *(corporate author)* issuing the report.

2a. REPORT SECURITY CLASSIFICATION: Enter the overall security classification of the report. Indicate whether "Restricted Data" is included. Marking is to be in accordance with appropriate security regulations.

2b. GROUP: Automatic downgrading is specified in DoD Directive 5200.10 and Armed Forces Industrial Manual. Enter the group number. Also, when applicable, show that optional markings have been used for Group 3 and Group 4 as authorized.

3. REPORT TITLE: Enter the complete report title in all capital letters. Titles in all cases should be unclassified. If a meaningful title cannot be selected without classification, show title classification in all capitals in parenthesis immediately following the title.

4. DESCRIPTIVE NOTES: If appropriate, enter the type of report, e.g., interim, progress, summary, annual, or final. Give the inclusive dates when a specific reporting period is covered.

5. AUTHOR(S): Enter the name(s) of author(s) as shown on or in the report. Enter last name, first name, middle initial. If military, show rank and branch of service. The name of the principal author is an absolute minimum requirement.

6. REPORT DATE: Enter the date of the report as day, month, year; or month, year. If more than one date appears on the report, use date of publication.

7a. TOTAL NUMBER OF PAGES: The total page count should follow normal pagination procedures, i.e., enter the number of pages containing information.

7b. NUMBER OF REFERENCES: Enter the total number of references cited in the report.

8a. CONTRACT OR GRANT NUMBER: If appropriate, enter the applicable number of the contract or grant under which the report was written.

8b, 8c, & 8d. PROJECT NUMBER: Enter the appropriate military department identification, such as project number, subproject number, system numbers, task number, etc.

9a. ORIGINATOR'S REPORT NUMBER(S): Enter the official report number by which the document will be identified and controlled by the originating activity. This number must be unique to this report.

9b. OTHER REPORT NUMBER(S): If the report has been assigned any other report numbers *(either by the originator or by the sponsor)*, also enter this number(s).

10. AVAILABILITY/LIMITATION NOTICES: Enter any limitations on further dissemination of the report, other than those imposed by security classification, using standard statements such as:

(1) "Qualified requesters may obtain copies of this report from DDC."

(2) "Foreign announcement and dissemination of this report by DDC is not authorized."

(3) "U. S. Government agencies may obtain copies of this report directly from DDC. Other qualified DDC users shall request through _____."

(4) "U. S. military agencies may obtain copies of this report directly from DDC. Other qualified users shall request through _____."

(5) "All distribution of this report is controlled. Qualified DDC users shall request through _____."

If the report has been furnished to the Office of Technical Services, Department of Commerce, for sale to the public, indicate this fact and enter the price, if known.

11. SUPPLEMENTARY NOTES: Use for additional explanatory notes.

12. SPONSORING MILITARY ACTIVITY: Enter the name of the departmental project office or laboratory sponsoring *(paying for)* the research and development. Include address.

13. ABSTRACT: Enter an abstract giving a brief and factual summary of the document indicative of the report, even though it may also appear elsewhere in the body of the technical report. If additional space is required, a continuation sheet shall be attached.

It is highly desirable that the abstract of classified reports be unclassified. Each paragraph of the abstract shall end with an indication of the military security classification of the information in the paragraph, represented as *(TS), (S), (C), or (U)*.

There is no limitation on the length of the abstract. However, the suggested length is from 150 to 225 words.

14. KEY WORDS: Key words are technically meaningful terms or short phrases that characterize a report and may be used as index entries for cataloging the report. Key words must be selected so that no security classification is required. Identifiers, such as equipment model designation, trade name, military project code name, geographic location, may be used as key words but will be followed by an indication of technical context. The assignment of links, roles, and weights is optional.

DD FORM 1 JAN 64 1473 (BACK)

DISTRIBUTION LIST

Documents Department
General Library
University of California
Berkeley, California 94720

Lockheed-California Company
Centeral Library
Dept. 77-14, Bldg. 170, Plt. B-1
Burbank, California 91503

Naval Ordnance Test Station
China Lake, California
Attn: Technical Library

Serials Dept., Library
University of California, San Diego
La Jolla, California 92038

Aircraft Division
Douglas Aircraft Company, Inc.
3855 Lakewood Boulevard
Long Beach, California 90801
Attn: Technical Library

Librarian
Government Publications Room
University of California
Los Angeles, California 90024

Librarian
Numerical Analysis Research
University of California
405 Hilgard Avenue
Los Angeles, California 90024

Chief Scientist
Office of Naval Research
Branch Office
1030 East Green Street
Pasadena, California 91101

Commanding Officer and Director
U. S. Navy Electronics Lab. (Library)
San Diego, California 92152

General Dynamics/Convair
P.O. Box 1950
San Diego, California 92112
Attn: Engineering Library
Mail Zone 6-157

Ryan Aeronautical Company
Attn: Technical Information
Services
Lindbergh Field
San Diego, California 92112

General Electric Company
Technical Information Center
P.O. Drawer QQ
Santa Barbara, California 93102

Library
Boulder Laboratories
National Bureau of Standards
Boulder, Colorado 80302

Government Documents Division
University of Colorado Libraries
Boulder, Colorado 80304

The Library
United Aircraft Corporation
400 Main Street
East Hartford, Connecticut 06108

Documents Division
Yale University Library
New Haven, Connecticut 06520

Librarian
Bureau of Naval Weapons
Washington, D. C. 20360

George Washington University Library
2023 G Street, N. W.
Washington, D. C. 20006

National Bureau of Standards Library
Room 301, Northwest Building
Washington, D. C. 20234

Director
Naval Research Laboratory
Washington, D. C. 20390
Attn: Code 2027

University of Chicago Library
Serial Records Department
Chicago, Illinois 60637

Documents Department
Northwestern University Library
Evanston, Illinois 60201

The Technological Institute, Library
Northwestern University
Evanston, Illinois 60201

Librarian
Purdue University
Lafayette, Indiana 47907

Johns Hopkins University Library
Baltimore
Maryland 21218

Martin Company
Science-Technology Library
Mail 398
Baltimore, Maryland 21203

Scientific and Technical Information
Facility
Attn: NASA Representative
P.O. Box 5700
Bethesda, Maryland 20014

Documents Office
University of Maryland Library
College Park, Maryland 20742

The Johns Hopkins University
Applied Physics Laboratory
Silver Spring, Maryland
Attn: Document Librarian

Librarian
Technical Library, Code 245L
Building 39/3
Boston Naval Shipyard
Boston, Massachusetts 02129

Massachusetts Institute of Technology
Serials and Documents
Hayden Library
Cambridge, Massachusetts 02139

Technical Report Collection
303A, Pierce Hall
Harvard University
Cambridge, Massachusetts 02138
Attn: Mr. John A. Harrison, Librarian

Alumni Memorial Library
Lowell Technological Institute
Lowell, Massachusetts

Librarian
University of Michigan
Ann Arbor, Michigan 48104

Gifts and Exchange Division
Walter Library
University of Minnesota
Minneapolis, Minnesota 55455

Reference Department
John M. Olin Library
Washington University
6600 Millbrook Boulevard
St. Louis, Missouri 63130

Librarian
Forrestal Research Center
Princeton University
Princeton, New Jersey 08540

U. S. Naval Air Turbine Test Station
Attn: Foundational Research Coordinator
Trenton, New Jersey 08607

Engineering Library
Plant 25
Grumman Aircraft Engineering Corp.
Bethpage, L. I., New York 11714

Librarian
Fordham University
Bronx, New York 10458

U. S. Naval Applied Science Laboratory
Technical Library
Building 291, Code 9832
Naval Base
Brooklyn, New York 11251

Librarian
Cornell Aeronautical Laboratory
4455 Genesee Street
Buffalo, New York 14225

Central Serial Record Dept.
Cornell University Library
Ithaca, New York 14850

Columbia University Libraries
Documents Acquisitions
535 W. 114 Street
New York, New York 10027

Engineering Societies Library
345 East 47th Street
New York, New York 10017

Library-Serials Department
Rensselaer Polytechnic Institute
Troy, New York 12181

Librarian
Documents Division
Duke University
Durham, North Carolina 27706

Ohio State University Libraries
Serial Division
1858 Neil Avenue
Columbus, Ohio 43210

Commander
Philadelphia Naval Shipyard
Philadelphia, Pennsylvania 19112
Attn: Librarian, Code 249c

Steam Engineering Library
Westinghouse Electric Corporation
Lester Branch Postoffice
Philadelphia, Pennsylvania 19113

Hunt Library
Carnegie Institute of Technology
Pittsburgh, Pennsylvania 15213

Documents Division
Brown University Library
Providence, Rhode Island 02912

Central Research Library
Oak Ridge National Laboratory
Post Office Box X
Oak Ridge, Tennessee 37831

Documents Division
The Library
Texas A & M University
College Station, Texas 77843

Librarian
LTV Vought Aeronautics Division
P.O. Box 5907
Dallas, Texas 75222

Gifts and Exchange Section
Periodicals Department
University of Utah Libraries
Salt Lake City, Utah 84112

Defense Documentation Center (DDC)
Cameron Station
Alexandria, Virginia 22314
Attn: IRS (20 copies)

FOREIGN COUNTRIES

Engineering Library
Hawker Siddeley Engineering
Box 6001
Toronto International Airport
Ontario, Canada
Attn: Mrs. M. Newns, Librarian

Exchange Section
National Lending Library for
Science and Technology
Boston Spa
Yorkshire, England

The Librarian
Patent Office Library
25 Southampton Buildings
Chancery Lane
London W. C. 2., England

Librarian
National Inst. of Oceanography
Wormley, Godalming
Surrey, England

Dr. H. Tigerschiold, Director
Library
Chalmers University of Technology
Gibraltargatan 5
Gothenburg S, Sweden

TA7
.U62 Demetry
no.70 Application of the
Kalman filter...